Kobe University Repository : Kernel

PDF issue: 2025-12-05

# Acceptor-related low-energy photoluminescence from boron-doped Si nanocrystals

Sugimoto, Hiroshi
Fujii, Minoru
Fukuda, Masatoshi
Imakita, Kenji
Hayashi, Shinji

(Citation)
JOURNAL OF APPLIED PHYSICS,110(6):063528-063528

(Issue Date)
2011-09-15

(Resource Type)
journal article

(Version)
Version of Record

(URL)
https://hdl.handle.net/20.500.14094/90001576

KOBE UNIVERSITY

# Acceptor-related low-energy photoluminescence from boron-doped Si nanocrystals

Hiroshi Sugimoto, Minoru Fujii,[a] Masatoshi Fukuda, Kenji Imakita, and Shinji Hayashi
*Department of Electrical and Electronic Engineering, Graduate School of Engineering, Kobe University, Rokkodai, Nada, Kobe 657-8501, Japan*

(Received 22 July 2011; accepted 18 August 2011; published online 27 September 2011)

Boron (B) doped Si nanocrystals (Si-ncs) dispersed in hydrofluoric (HF) acid solution are prepared by dissolving borosilicate films containing B-doped Si-ncs in HF solution. We find that the etching rate of B-doped Si-ncs is much smaller than that of undoped Si-ncs. The difference of the etching rate allows us to extract only doped Si-ncs in the mixture of doped and undoped Si-ncs and observe the photoluminescence (PL) due to the transition from the conduction band to the acceptor state. The PL was very broad with the maximum around 1.15 eV. From the analysis of the PL data obtained for the samples prepared under different conditions and different etching time, preferential doping sites of B atoms are estimated. The data suggests that B-doped Si-ncs consists of intrinsic cores and heavily B-doped shells. © *2011 American Institute of Physics*. [doi:10.1063/1.3642952]

## I. INTRODUCTION

Si nanocrystals (Si-ncs) have attracted considerable research attention for more than a decade because of their potential applications in optoelectronics[1,2] and biology.[3,4] The optical and electrical transport properties of Si-ncs can be controlled by the size, shape and surface chemistry. In particular, the size-dependence of the optical properties has been extensively studied experimentally[5,6] and theoretically[7,8] and the mechanism of the near infrared (NIR) to visible luminescence has almost been clarified.[5–10]

For the application of Si-ncs in optoelectronic devices, controlling the carrier density by impurity doping is indispensable. There has been a lot of theoretical work on *n*- and/or *p*-type impurity-doped Si-ncs (Refs. 11–16). All of them demonstrate that the energy level structures are strongly modified by a very small number of impurity atoms. Furthermore, preferential doping sites and the formation energy of doped Si-ncs are calculated.[15,16] The formation energy is reported to be very large for doped Si-ncs.[11] The large formation energy indicates that Si-ncs tend to be intrinsic by pushing impurity atoms out during the growth and explains the so-called self-purification effect.[17] A problem still remaining is the effect of surface termination on the energy state structures of doped Si-ncs. All theoretical work performed so far on doped Si-ncs is concerning hydrogen (H)-terminated Si-ncs, and to our knowledge, no calculation has been done on doped oxygen (O)-terminated Si-ncs. On the other hand, the most stable surface of Si is Si-O bonds. Therefore, many of experimentally prepared doped Si-ncs have $SiO_2$ shells, or even if the surface is initially terminated by H atoms or organic molecules, after a certain period, they are partly replaced by O atoms. Since very small amount of O atoms on the surface is expected to modify the energy state structure of doped Si-ncs, theoretical study on the effect is highly demanded.

In contrast to the recent progress of theoretical studies of doped Si-ncs, the experimental ones are limited. This is mainly due to inhomogeneous broadening of experimental data because of the large distributions of sample parameters, such as the size, shape, defect density, impurity concentration, impurity sites, and so on and due to the lack of proper characterization techniques. Doped Si-ncs are mainly studied by photoluminescence (PL),[18–20] electron paramagnetic resonance (EPR),[21–23] and Raman spectroscopy.[23–25] PL properties of boron (B) and/or phosphorus (P) doped Si-ncs samples have been studied for Si-ncs in solid matrices[18,19] and those in powder form.[20] From the analysis of the PL properties, Pi *et al.*[20] assigned preferential doping sites of P or B in *in-situ* doped plasma-synthesized Si-ncs. In our previous work,[21] we studied the hyper-fine structure of EPR spectra of P-doped Si-ncs in glass matrices and demonstrated the evidence of the quantum confinement of donors in Si-ncs. Stegner *et al.*[22] studied P-doped Si-ncs powder by EPR spectroscopy and demonstrated that doping efficiency of Si-ncs decreases significantly when the diameter becomes smaller than 10 nm. For example, only about 0.2% of doped impurities are activated when the diameter is about 10 nm. This means that in Si-ncs assemblies, even if average doping concentration in the whole system is very high, only a fraction of Si-ncs have active impurities.

The very small doping efficiency exerts a serious problem when we study PL properties of doped Si-ncs. The PL quantum efficiency of doped Si-ncs is expected to be more than three orders of magnitude smaller than that of intrinsic Si-ncs because of the strong Auger interaction between photoexcited excitons and carriers supplied by doped impurities.[26] Therefore, the PL spectra of doped Si-ncs samples are almost totally controlled by undoped Si-ncs if small fraction of them remains in the samples and those from doped Si-ncs are hard to be detected. As a result, PL spectral shape of doped Si-ncs samples studied so far is very similar to those reported for intrinsic Si-ncs samples except for small differences in the low-energy tail region.[27] In order to study the electronic state structures of doped Si-ncs by PL

[a]Author to whom correspondence should be addressed. Electronic mail: fujii@eedept.kobe-u.ac.jp.

 © 2011 American Institute of Physics

Downloaded 07 Nov 2011 to 133.30.52.203. Redistribution subject to AIP license or copyright; see http://jap.aip.org/about/rights_and_permissions

spectroscopy, samples consisting only of active impurity-doped Si-ncs are indispensable.

In this work, we demonstrate that extraction of active impurity-doped Si-ncs from Si-nc assemblies can be achieved by simply dissolving borosilicate glass (BSG) films containing B-doped Si-ncs by hydrofluoric acid (HF) solution. We show that PL spectra changes drastically by the etching and only the low energy region of the spectra attributable to doped Si-ncs remains. An advantage of this method is that H-termination is guaranteed because the samples are kept in HF solution. This can remove the uncertainty of the data caused by partial oxidation of the surface. From the comparison of the PL data between doped and undoped Si-ncs samples and from the effect of air exposure of the etched samples to PL spectra, we will discuss the preferential doping sites of B atoms in Si-ncs.

## II. EXPERIMENTAL PROCEDURE

$SiO_2$ films containing Si-ncs were prepared by a cosputtering method.[18,24] For intrinsic Si-ncs, small pieces of Si chips ($10 \times 15$ mm$^2$) were placed on a $SiO_2$ sputtering target (10 cm in diameter) and they were simultaneously sputtered in Ar gas of 2.7 Pa. For B-doped Si-ncs, Si chips ($10 \times 15$ mm$^2$) and $B_2O_3$ pellets (10 mm in diameter) were placed on a $SiO_2$ sputtering target. Fused silica plates were used as a substrate for the growth of thin film samples. To prepare powder samples, the films were deposited on stainless steel plates and peeled from the plates just after the sputtering. The films and powder were annealed at the temperature of 1150 to 1250 °C in a $N_2$ gas atmosphere for 30 min to grow Si-ncs in $SiO_2$ or in BSG matrices. The average concentration of $B_2O_3$ in a sample was estimated from the intensity ratio of the B-O ($\sim$1400 cm$^{-1}$) and Si-O ($\sim$1080 cm$^{-1}$) vibration peaks in the IR absorption spectra.[28] The B concentration [$C_B$ (at.%)] calculated from the ratio of $SiO_2$, $B_2O_3$ and excess Si was about 0.75 at.% for all the samples studied in this work. Note that the concentration is an average concentration in the whole film and is not that in Si-ncs.

In order to isolate Si-ncs from matrices, the powder samples were crushed in a mortar and 3 mg of it was dispersed in HF solution (46 wt.%, 1.5 mL) in a polymethylmethacrylate (PMMA) cell. The amount of HF is more than enough to completely dissolve $SiO_2$ or BSG matrices of the 3 mg samples. Photoluminescence spectra were measured in the HF solution. The solution was continuously stirred by a magnetic stirrer during the etching and measurements. Photoluminescence spectra of thin film samples were collected from the sample by a conventional PL setup. The photoluminescence was analyzed by using a single spectrometer and detected by a liquid-nitrogen cooled InGaAs diode array. The excitation source was a 488.0 nm line of an Ar ion laser or a 405 nm diode laser. The spectral response of the detection system was corrected with a reference spectrum of a standard halogen lamp. Photoluminescence decay curves were measured using a near infrared photomultiplier tube (R5509-72, Hamamatsu Photonics) and a multi-channel scaler (SR430, Stanford Research). All the measurements were performed at room temperature.

## III. RESULTS AND DISCUSSION

### A. B-doped Si nanocrystals in glass matrices

Before discussing PL properties of isolated B-doped Si-ncs, we summarize that of intrinsic and B-doped Si-ncs in solid matrices. The average diameters of the intrinsic and B-doped Si-ncs in the matrices estimated by transmission electron microscopy (TEM) observations are 4–5 nm. Figure 1(a) compares PL spectral shape of intrinsic and B-doped samples exhibiting the PL maximum around 1.4 eV. Although the spectral shape is very similar at the high-energy side, we can see a clear difference at the low-energy side; the B-doped sample has a broad tail below the bandgap energy of bulk Si crystal, while the intrinsic sample does not. Since the tail appears by doping, it is considered to arise from the optical transitions involving the acceptor states.

Figure 1(b) compares PL decay curves of intrinsic and B-doped samples detected at 1.2 eV. The decay curve of the intrinsic sample consists of a fast and a slow components. The PL decay behavior of intrinsic Si-ncs has been studied in detail.[6] It has been shown that the slow component exhibits strong size, i.e., detection energy, dependence and it becomes fast with decreasing the size. From the size dependence and the temperature dependence of the decay time,[6] the slow component is usually assigned to the radiative recombination of quantum confined excitons.[6] The shortening of the exciton lifetime with decreasing the size is considered to be due to better overlap of electron and hole wavefunctions in

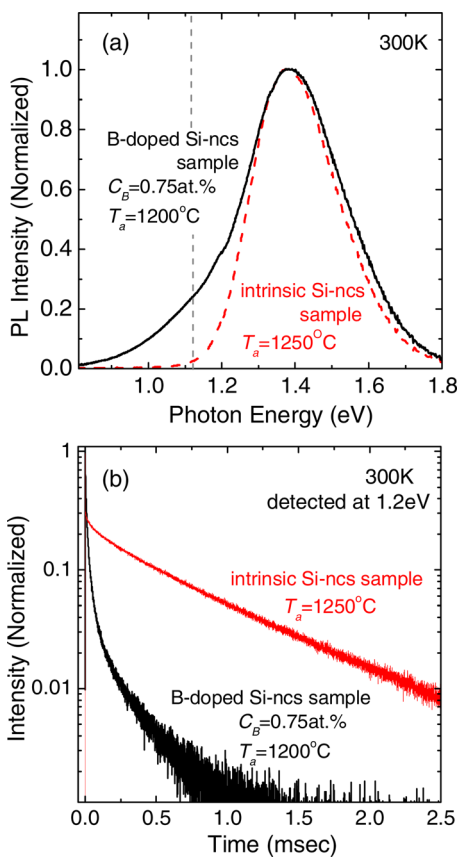


FIG. 1. (Color online) (a) Normalized PL spectra of thin film form intrinsic and B-doped Si-ncs samples. (b) PL decay curves detected at 1.2 eV.

Downloaded 07 Nov 2011 to 133.30.52.203. Redistribution subject to AIP license or copyright; see http://jap.aip.org/about/rights_and_permissions

the momentum space.[29] On the other hand, the fast component does not show clear size dependence and is sometimes observed even below the bulk Si bandgap. This suggests that the fast component is due to defects in or on the surface of Si-ncs. Compared to the intrinsic sample, the PL decay time of the B-doped sample is much shorter. The decay time obtained by fitting the decay curve by a stretched exponential function is 10 $\mu$sec.

Figures 2(a) and 2(b) show PL spectra of intrinsic and B-doped samples, respectively, excited in the power range from 70 mW to 2.0 W. In the intrinsic Si-ncs, we can see the high-energy shift of the peak when the excitation power is increased. This is due to different exciton lifetimes at different photon energies; PL from larger size Si-ncs in a size distribution saturates easier than that from smaller size Si-ncs because of the longer exciton lifetime. Similar high-energy shift of the peak is observed for the B-doped sample [Fig. 2(b)]. The difference between the intrinsic and B-doped samples appears at the low-energy side of the spectrum. In B-doped Si-ncs, a new band emerges in the low-energy region when the excitation power is increased. In the inset of Fig. 2(b), the PL intensities at 1.1 and 1.4 eV are plotted as a function of the excitation power. We can see that the main band saturates stronger than the low-energy tail.

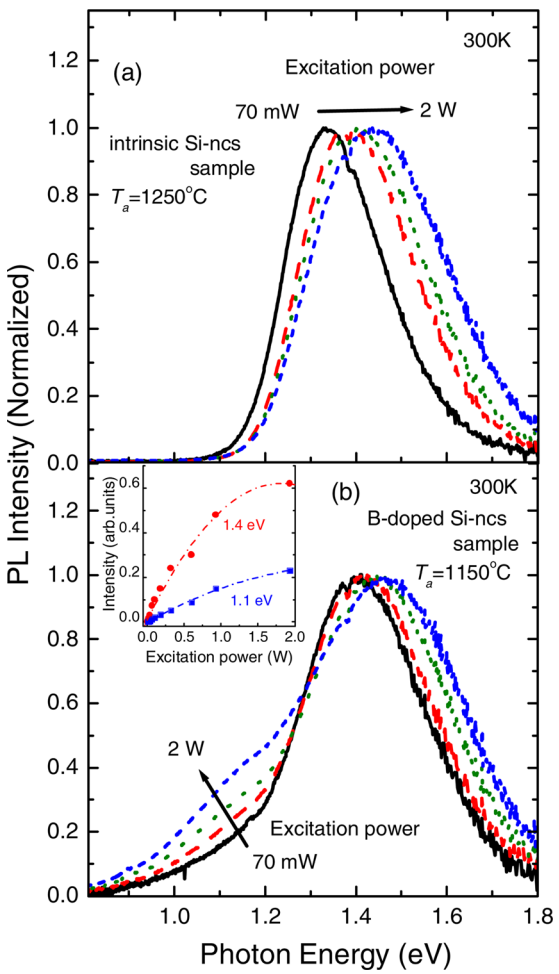


FIG. 2. (Color online) Excitation power dependence of normalized PL spectra of thin film form (a) intrinsic and (b) B-doped Si-ncs samples. Inset: PL intensities of B-doped Si-ncs sample as a function of excitation power.

The different excitation power dependence between the high-and low-energy regions suggests that Si-ncs in B-doped samples consist of two groups. One group is Si-ncs contributing to the PL in the high-energy region. In this group, B is considered to be not doped or not activated because the excitation power dependence of the PL is very similar to that of the intrinsic samples. The other group is Si-ncs with electrically-active B. These nanocrystals show fast PL in the low-energy region due to the optical transitions involving the acceptor states. The lifetime is consider to be determined mainly by the nonradiative Auger process between holes supplied by B doping and photoexcited excitons.

### B. B-doped Si nanocrystals in HF solution

Before conducting optical measurements, we studied Si-ncs after HF etching by TEM. For TEM observations, samples were washed several times to remove HF and dispersed in methanol. The solution was then dropped on carbon-coated copper grids. Figure 3 shows a TEM image of B-doped Si-ncs dispersed in methanol after HF etching for 30 min. We can see lattice fringes corresponding to the {111} planes of Si-ncs. The average diameter is about 4.5 nm with the standard deviation of 1.3 nm. From the image, we can confirm that Si-ncs are isolated from matrices.

Figure 4(a) shows PL spectra of an intrinsic sample before and during the HF etching. The PL before the etching is measured by dispersing the crushed fine powder (3 mg) in methanol, while that during etching is measured by dispersing the same amount of powder in HF solution by the procedure written above. Before the etching, the PL peak appears at 1.45 eV. By the HF etching, the spectrum shifts to the higher energy and the intensity decreases; the 10 min etching results in the shift of the PL maximum to 1.55 eV. This shift is explained by modification of the surface termination from O to H and by the size decrease.[10] The intensity decrease is due to defect formation on the surface of Si-ncs by etching and also due to induced surface charges because of the dispersion of Si-ncs in polar liquid. Photoluminescence quenching in polar solvents have been reported for porous Si (Ref. 30). When the sample is etched longer, the PL shifts and quenches further. This is probably due to size decrease by laser irradiation in high concentration HF solution.[31]

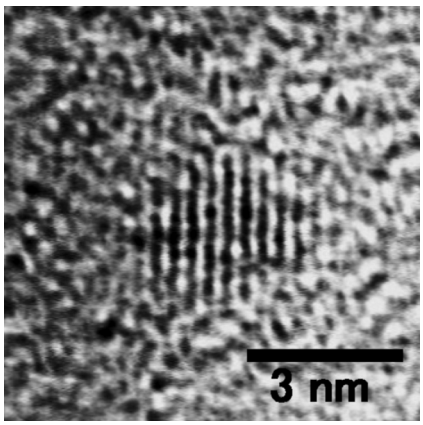


FIG. 3. High-resolution TEM image of B-doped Si-ncs after HF etching.

Downloaded 07 Nov 2011 to 133.30.52.203. Redistribution subject to AIP license or copyright; see http://jap.aip.org/about/rights_and_permissions

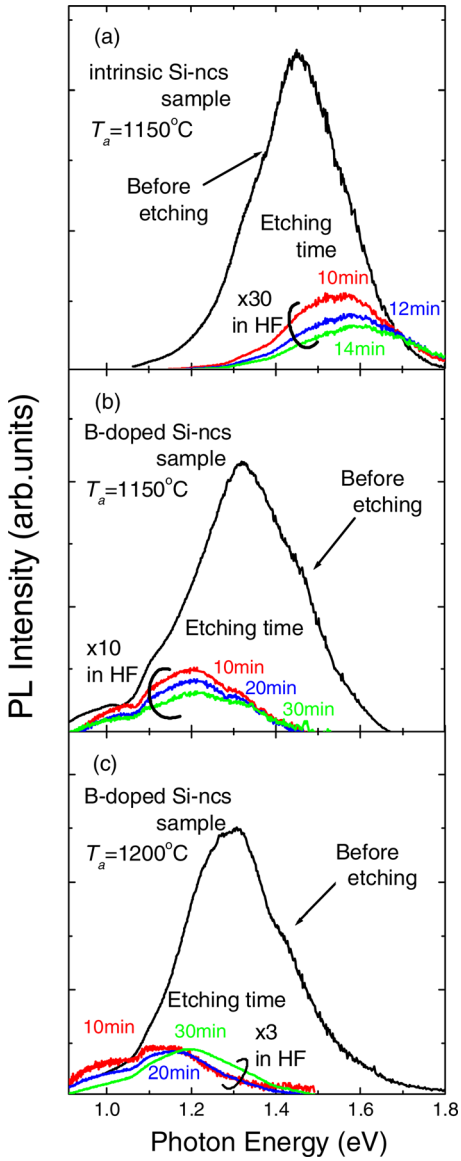


FIG. 4. (Color online) PL spectra taken before and during HF etching. The etching time is indicated in the graphs. (a) Intrinsic Si-ncs samples annealed at 1150 °C, (b) B-doped Si-ncs samples annealed at 1150 °C, and (c) B-doped Si-ncs samples annealed at 1200 °C.

Figures 4(b) and 4(c) show PL spectra of B-doped samples annealed at 1150 and 1200 °C, respectively. Before the etching, B-doped samples exhibit a broad PL band with the maximum around 1.3 eV. A dip around 1.06 eV is due to absorption of emitted light by O-H stretching vibrations of water and by a PMMA cell. After the HF etching, in both samples, only the low-energy-tail region remains and the main band disappears. As a result, the PL peak shifts to lower energy. In Fig. 2, we proposed a model that the B-doped samples consist of Si-ncs with active B atoms and those in which B atoms are not doped. The former exhibits short-lifetime PL in the low-energy region, while the latter long-lived PL in the high-energy region. Figures 4(b) and 4(c) suggest that after the HF etching, only B-doped Si-ncs remain in the HF solution, and the PL due to the electronic transition between the conduction band and the acceptor states emerges.

The PL spectral shape of B-doped Si-ncs remaining after the etching is qualitatively different from that of intrinsic Si-ncs. In general, intrinsic Si-ncs have a PL cutoff at the bandgap energy of bulk Si crystal.[6] On the other hand, PL from the B-doped Si-ncs extends deep below the bulk Si bandgap. This is another evidence that the acceptor states are involved in the optical transition. Figure 5(a) shows PL peak energies as a function of the etching time. The PL peak energy of the sample annealed at 1200 °C is lower than that of the sample annealed at 1150 °C. In both samples, the peak shifts to higher energy with increasing the etching time. However, the shift is much smaller than that observed for the intrinsic sample. In general, the energy levels of hydrogenic impurities are less sensitive to the size of Si-ncs because of the small effective Bohr radius.[32] Therefore, the conduction band to acceptor states transition reflects only the shift of the conduction bandedge when the size is changed, and thus the shift is smaller than that of the band-to-band transitions. The different PL peak energies between the samples annealed at 1150 °C and 1200 °C after etching are considered to reflect the size difference.

Figure 5(b) shows the PL intensity as a function of the etching time. Before the etching, the PL intensities of B-doped samples are much smaller than that of the intrinsic sample. The small PL intensity is due to the Auger recombination of photoexcited carriers with the interaction with holes supplied by B doping.[33] The PL intensities of both the intrinsic and B-doped samples decrease by the HF etching. However, the degree of the intensity decrease is different,

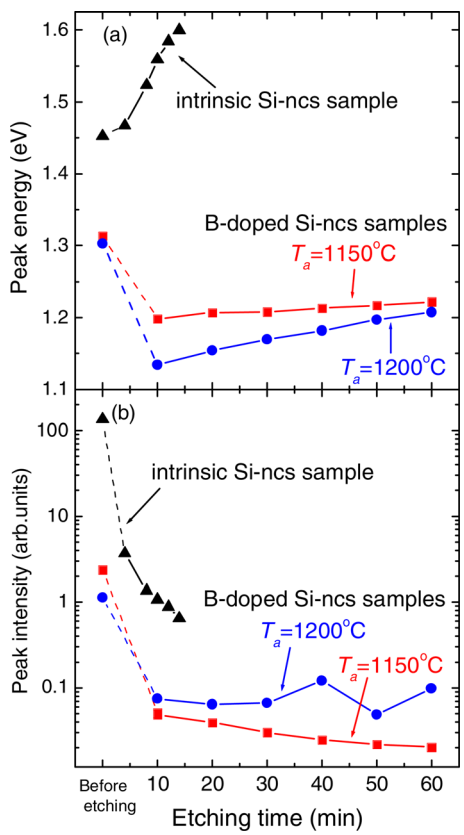


FIG. 5. (Color online) (a) PL peak energy and (b) peak intensity of intrinsic and B-doped Si-ncs samples as a function of the HF etching time.

Downloaded 07 Nov 2011 to 133.30.52.203. Redistribution subject to AIP license or copyright; see http://jap.aip.org/about/rights_and_permissions

i.e., the PL of the intrinsic sample quenches faster than that of doped samples. This suggests that B-doped Si-ncs are less vulnerable to HF than undoped Si-ncs. We will discuss the mechanism later.

In Fig. 5(b), it is interesting to note that, after the etching, the PL intensities of B-doped samples annealed at 1200 °C are larger than those of the sample annealed at 1150 °C, despite the smaller PL intensity before the etching. This can be explained by considering different ratio of active impurity-doped Si-ncs between the two samples. In the sample annealed at 1200 °C, many of Si-ncs are B-doped. As a result, initial PL intensity determined mainly by the number of undoped Si-ncs is smaller, while that after the etching determined by the number of doped Si-ncs is larger. It is vice versa, in the sample annealed at 1150 °C.

### C. Location of B in B-doped Si nanocrystals

Figures 4 and 5 strongly suggest that B-doped Si-ncs are less vulnerable to HF than undoped Si-ncs. A possible explanation of this effect is that B is doped near the surface of Si-ncs. It is well known that the segregation coefficient of B at the $Si/SiO_2$ interface is small (~0.3) (Ref. 34). Therefore, during the growth of Si-ncs in $SiO_2$ by annealing, B atoms are precipitated near the interface. Since Si-B bonds are reported to be much more resistant to HF than Si-Si bonds,[35] if B atoms are doped in the sub-surface, the etching rate of B-doped Si-ncs is expected to be much smaller than that of intrinsic Si-ncs.

In order to confirm the model that B atoms are doped in the sub-surface of Si-ncs, we performed the following experiments. After etching 30 min in HF solution, the samples were washed and stored in methanol. The PL spectra of the samples in methanol are shown in Fig. 6(a) with that of the sample before etching. The spectra are normalized at the maximum intensity. The PL spectrum of the sample kept one day in methanol is very similar to that in HF solution in Fig. 4(c). The dip at 1.03 eV is attributable to absorption of emitted light by the overtones of C-H stretching vibrations of methanol. The spectral shape changes drastically by keeping the sample 16 days in methanol. The PL peak returns almost to the original position before the etching and the spectral shape is very similar to that of intrinsic Si-ncs samples. After three months, although further drastic change of the spectral shape is not observed, the intensity below the bandgap energy of bulk Si crystal continuously decreases and almost disappears. The drastic change of the PL spectrum suggests that active B atoms in B-doped Si-ncs are inactivated by just keeping the samples in methanol. In order to confirm that B atoms are inactivated, we measured PL lifetimes of the samples kept three months in methanol and compared them with those of an intrinsic sample. Figure 6(b) shows the PL lifetimes as a function of the detected photon energy. The inset shows the PL decay curve of the B-doped sample at 1.2 eV. The decay curve is completely different from that shown in Fig. 1(b). The decay curve is a single exponential function and the lifetime is about 360 $\mu$sec. The lifetime is very close to that of the intrinsic sample in the whole energy range studied. Therefore, B is indeed inactivated in methanol at room temperature. This strongly suggests that active B atoms exist very close to the surface of Si-ncs.

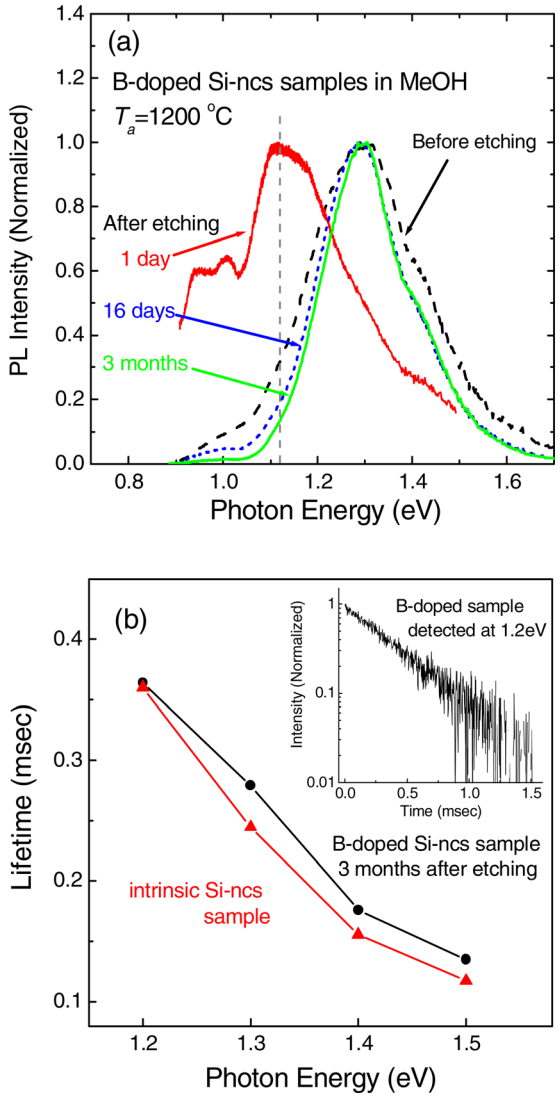


FIG. 6. (Color online) (a) Normalized PL spectra of B-doped Si-ncs samples measured in methanol before HF etching and kept one day, 16 days and 3 months in methanol after HF etching. The HF etching time is 30 min. (b) PL lifetimes of the sample kept three months in methanol and an intrinsic sample as a function of photon energy. Inset: PL decay curve of the sample kept three months in methanol detected at 1.2 eV.

The most plausible explanation of the room temperature inactivation of B atoms is the oxidation of the Si-nc surface. In H-terminated Si-ncs, the Si-Si back-bonds are easily oxidized in air or in water at room temperature. In the present samples, when they are kept in HF solution, the surface is always H-terminated. If the samples are kept in methanol for a long period, the Si-Si bonds below the Si-B bonds are oxidized and B atoms are incorporated into surface oxide layers. This results in inactivation of B and drastic change of the PL spectra.

## IV. CONCLUSION

We have succeeded in observing the acceptor state related PL from B-doped Si-ncs. We found that B-doped Si-ncs consist of a high B concentration shell and an intrinsic core and the shell prevents etching of doped Si-ncs from HF.

Downloaded 07 Nov 2011 to 133.30.52.203. Redistribution subject to AIP license or copyright; see http://jap.aip.org/about/rights_and_permissions

This structure allows us to extract B-doped Si-ncs from the assembly of doped and undoped Si-ncs and observe the PL from H-terminated B-doped Si-ncs. The B-doped Si-ncs show a very broad PL with the maximum around 1.1 to 1.2 eV. The large width is considered to be due to the distributions of the size of Si-ncs and number of active B atoms in Si-ncs. Further detailed studies are required to fully understand the relation between the PL spectra and these parameters. The present result is also important from the application point of view. Since B atoms exist very close to the surface of Si-ncs, they are very easily deactivated by oxidation at room temperature. To avoid the effect, B-doped Si-ncs should be kept in oxygen-free environment until used as source materials for optoelectronic devices.

## ACKNOWLEDGMENTS

This work is supported in part by a Grant-in-Aid for Scientific Research from the Ministry of Education, Culture, Sports, Science and Technology, Japan and by Research Grants in the Natural Sciences from Mitsubishi Foundation.

[1]L. Brus, *Semiconductor and Semimetals*, edited by D. J. Lockwood (Academic, New York, 1998), Vol. 49, p. 303.
[2]O. Bisi, S. Ossicini, and L. Pavesi, Surf. Sci. Rep. **38**, 1 (2000).
[3]F. Erogbogbo, K. Yong, I. Roy, G. Xu, P. Prasad, and M. Swihart, ACS Nano **2**, 873 (2008).
[4]J. Park, L. Gu, G. von Maltzahn, E. Ruoslahti, S. Bhatia, and M. Sailor, Nature Mater. **8**, 331 (2009).
[5]D. Kovalev, H. Heckler, G. Polisski, and F. Koch, Phys. Status Solidi B **215**, 871 (1999).
[6]S. Takeoka, M. Fujii, and S. Hayashi, Phys. Rev. B **62**, 016820 (2000).
[7]C. Delerue, G. Allan, and M. Lannoo, Phys. Rev. B **48**, 011024 (1993).
[8]V. A. Belyakov, V. A. Burdov, R. Lockwood, and A. Meldrum, Adv. Opt. Technol. **2008**, 279502 (2008).
[9]G. Ledoux, O. Guillois, D. Porterat, C. Reynaud, F. Huisken, B. Kohn, and V. Paillard, Phys. Rev. B **62**, 015942 (2000).
[10]M. Wolkin, J. Jorne, P. Fauchet, G. Allan, and C. Delerue, Phys. Rev. Lett. **82**, 197 (1999).
[11]S. Ossicini, E. Degoli, F. Iori, E. Luppi, R. Magri, G. Cantele, F. Trani, and D. Ninno, Appl. Phys. Lett. **87**, 173120 (2005).
[12]F. Iori, E. Degoli, R. Magri, I. Marri, G. Cantele, D. Ninno, F. Trani, O. Pulci, and S. Ossicini, Phys. Rev. B **76**, 085302 (2007).
[13]Q. Xu, J. Luo, S. Li, J. Xia, J. Li, and S. Wei, Phys. Rev. B **75**, 235304 (2007).
[14]E. de Oliveira, E. Albuquerque, J. de Sousa, and G. Farias, Appl. Phys. Lett. **94**, 103114 (2009).
[15]X. Chen, X. Pi, and D. Yang, J. Phys. Chem. C **115**, 661 (2011).
[16]J. Eom, T. Chan, and J. Chelikowsky, Solid State Commun. **150**, 130 (2010).
[17]G. Dalpian and J. Chelikowsky, Phys. Rev. Lett. **96**, 226802 (2006).
[18]M. Fujii, S. Hayashi, and K. Yamamoto, J. Appl. Phys. **83**, 7953 (1998).
[19]M. Fujii, A. Mimura, S. Hayashi, and K. Yamamoto, Appl. Phys. Lett. **75**, 184 (1999).
[20]X. Pi, R. Gresback, R. Liptak, S. Campbell, and U. Kortshagen, Appl. Phys. Lett. **92**, 123102 (2008).
[21]M. Fujii, A. Mimura, S. Hayashi, Y. Yamamoto, and K. Murakami, Phys. Rev. Lett. **89**, 206805 (2002).
[22]A. Stegner, R. Pereira, R. Lechner, K. Klein, H. Wiggers, M. Stutzmann, and M. Brandt, Phys. Rev. B **80**, 165326 (2009).
[23]R. Lechner, A. Stegner, R. Pereira, R. Dietmueller, M. Brandt, A. Ebbers, M. Trocha, H. Wiggers, and M. Stutzmann, J. Appl. Phys. **104**, 053701 (2008).
[24]Y. Kanzawa, M. Fujii, S. Hayashi, and K. Yamamoto, Solid State Commun. **100**, 227 (1996).
[25]K. Sato, N. Fukata, and K. Hirakuri, Appl. Phys. Lett. **94**, 161902 (2009).
[26]C. Delerue, M. Lannoo, G. Allan, E. Martin, I. Mihalcescu, J. Vial, R. Romestain, F. Muller, and A. Bsiesy, Phys. Rev. Lett. **75**, 2228 (1995).
[27]M. Fujii, Y. Yamaguchi, Y. Takase, K. Ninomiya, and S. Hayashi, Appl. Phys. Lett. **85**, 1158 (2004).
[28]A. Tenney, J. Electrochem. Soc. **118**, 1658 (1971).
[29]M. Fujii, Y. Yamaguchi, Y. Takase, K. Ninomiya, and S. Hayashi, Appl. Phys. Lett. **87**, 211919 (2005).
[30]J. Lauerhaas, G. Credo, J. Heinrich, and M. Sailor, J. Am. Chem. Soc. **114**, 1911 (1992).
[31]C. Choy and K. Cheah, Appl. Phys. A **61**, 45 (1995).
[32]C. Delerue, M. Lannoo, G. Allan, and E. Martin, Thin Solid Films **255**, 27 (1995).
[33]A. Mimura, M. Fujii, S. Hayashi, and K. Yamamoto, Solid State Commun. **109**, 561 (1999).
[34]S. M. Sze, *Physics of Semiconductor Devices,* 2nd ed. (Wiley, New York, 1981).
[35]G. Polisski, H. Heckler, D. Kovalev, M. Schwartzkopff, and F. Koch, Appl. Phys. Lett. **73**, 1107 (1998).

Downloaded 07 Nov 2011 to 133.30.52.203. Redistribution subject to AIP license or copyright; see http://jap.aip.org/about/rights_and_permissions